SUPPORTING INFORMATION

Organic Amorphous Hole-Transporting Materials Based on Tröger's Base: Alternatives to NPB

Ishita Neogi,[a] Samik Jhulki,[a] Madhu Rawat,[b] R. S. Anand,[b] Tahsin J. Chow[c] and Jarugu Narasimha Moorthy[a,*]

[a]*Department of Chemistry, Indian Institute of Technology, Kanpur 208016, INDIA*
[b]*Department of Electrical Engineering, Indian Institute of Technology, Kanpur 208016, INDIA*
[c]*Institute of Chemistry, Academia Sinica, Taipei, Taiwan 115, Republic of China*

E-Mail: *moorthy@iitk.ac.in*

Table of Contents

EXPERIMENTAL SECTION

General Aspects. All Pd mediated C-N and C-C coupling reactions were performed under a nitrogen gas atmosphere in oven-dried pressure tubes. ^{1}H and ^{13}C NMR spectra were recorded on JEOL (400 and 500 MHz) spectrometer in $CDCl_3$ as a solvent. The ESI mass spectra were recorded on Waters ^{Q}TOF machine. IR spectra were recorded on a Bruker Vector 22 FT-IR spectrophotometer. X-ray powder patterns were recorded on Rigaku X-ray diffractometer. The TGA and DSC measurements were carried out using Perkin-Elmer and Mettler-Toledo at 10 ^{o}C/min under a nitrogen gas atmosphere. UV-Vis absorption spectra were recorded using a Shimadzu UV-1800 spectrophotometer and PL measurements in solution and solid state were done using FluoroMax-4; FM4-3000 spectrofluorometer. Cyclic voltammetry measurements were done using CHI610E electrochemical work-station (CH instruments, Texas, USA). All the reactions were monitored by analytical thin layer chromatography (TLC) using commercial aluminum sheets pre-coated with silica gel.

Materials. The starting materials, viz., 2,8-dibromo-6*H*,12*H*-5,11-methanodi-benzo[*b*,*f*][1,5]-diazocine (2,8-dibromoTB), 2,8-dibromo-4,10-dimethyl-6*H*,12*H*-5,11-methanodi-benzo[*b*,*f*][1,5]-diazocine (2,8-dibromo-4,10-dimethylTB) were synthesized according to the literature reported procedures.[1]

PL Quantum Yield Measurements (Solution State). For determination of fluorescence quantum yields, the solutions of anthryl-**TB**s were prepared in dichloromethane (spectral grade). Quantum yields were calculated by exciting the solutions at 340 nm using anthracene as standard. The quantum yield was calculated from the following relation:

$$\Phi_u = \Phi_s(A_s/A_u)\,(I_u/I_s)\,(\eta_u/\eta_s)^2$$

where the subscripts s and u refer to standard and unknown samples, A_u and A_s to absorbances of the sample and the standard at the excitation wavelength, I_u and I_s to the integrated emission intensities (i.e., areas under the emission curves) of the sample and the standard and η_u and η_s to the refractive indices of the corresponding solutions (pure solvents are assumed).

Electrochemical Measurements. The cyclic voltammetry experiments were performed on an electrochemical analyzer, and the data were collected and analyzed using electrochemical analysis software. All experiments were carried out in a three electrode compartment cell using a Ag/AgCl reference electrode, a Pt wire counter electrode and a Pt working electrode. Instrument was first calibrated using Ferrocene/ferrocenium (Fc/Fc^+) redox couple (HOMO = –4.8 eV with respect to vacuum). The (Fc/Fc^+) redox couple displayed a half cell potential of 0.45 V. The supporting electrolyte used was 0.1 M tetrabutylammonium hexafluorophosphate solution in dry dichloromethane and the cell containing the solution of the sample (1mM) and the supporting electrolyte was purged with a nitrogen gas thoroughly before scanning for its oxidation and reduction properties. The oxidation and reduction potentials of all **TB**s were subsequently calculated from onset oxidation potentials. The HOMO energy in each case was calculated with reference to the ferrocene oxidation potential by using the following general equation:

$$E_{HOMO} = -[(E_{onset(ox)} - E_{1/2,Fc/Fc+}) + 4.8 \text{ eV}]$$

The LUMO energies were obtained by subtraction of the band gap enegries from the HOMO energies. The band gap energies for the compounds were calculated from the long range absorption cut-off wavelength.

$$E_{LUMO} = E_{HOMO} - E_g^{opt}$$

Device Fabrications. Device Fabrication. The patterned ITO-coated glass slides were cleaned rigorously by sonication sequentially in detergent solution, distilled water (4 times), isopropanol and acetone for 15 min each. Subsequently, they were dried in a flow of nitrogen and further cleaned by three cycles of oxygen plasma treatment (All Real Tech. PCD150) at 45 W for 5 min. The cleaned ITO-coated glasses were transferred to a vacuum chamber (10^{-5} to 10^{-6} torr), and placed in a rotating holder firmly. Organic layers and metals were deposited at a rate of 0.4–1.0 and 8-10 Å/s, respectively. The thickness of each layer was monitored by a quartz thickness controller placed near the rotating disk. After completion of the evaporation without breaking the vacuum, the devices were sealed by cover-glasses containing UV-cured epoxy glue at the periphery. The I-V-L characteristics and other measurements of the devices thus made were performed using a Keithly 2400 source meter connected to a PR650 spectrophotometer.

Synthesis of TB1-4

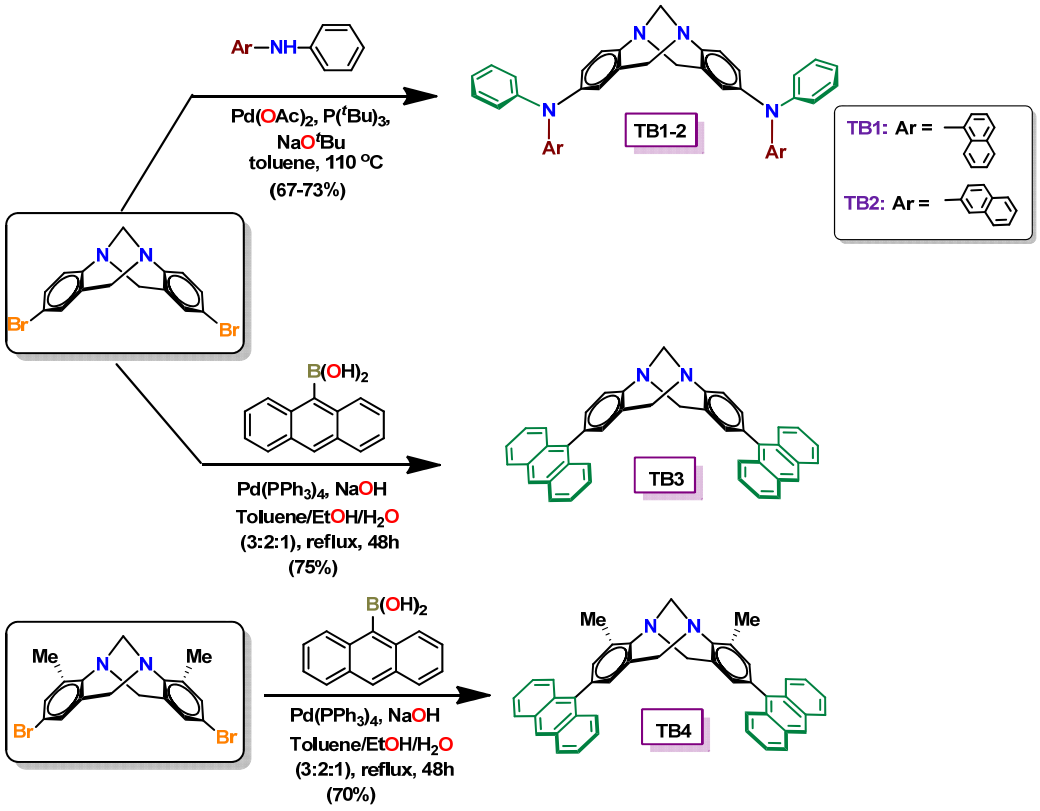

Scheme S1. Synthesis of **TB1-4**.

Synthesis of TB1

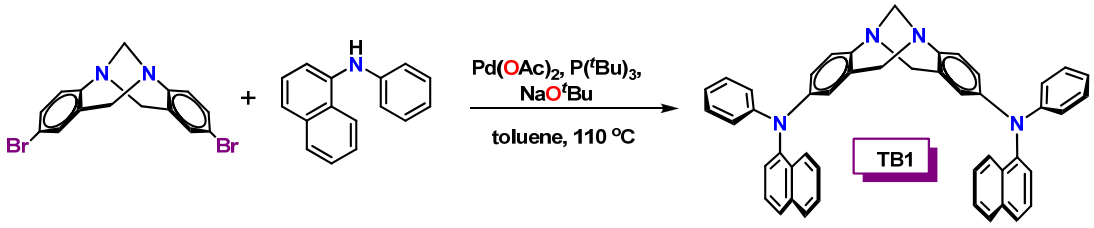

2,8-dibromo-substituted Tröger's base (2,8-dibromo-6*H*,12*H*-5,11-methanodibenzo[*b*,*f*][1,5]-diazocine) was synthesized by following the literature-reported procedure.[1] For C-N coupling reaction,[2] oven-dried pressure tube was cooled under nitrogen gas and charged with 2,8-dibromo-6*H*,12*H*-5,11-methanodi-benzo[*b*,*f*][1,5]-diazocine (0.30 g, 0.8 mmol), *N*-phenyl-1-naphthalenamine (0.41 g, 1.9 mmol), NaO^{t}Bu (0.08 g, 0.8 mmol), $Pd(OAc)_2$ (0.02 g, 10 mol%) and P(^{t}Bu)$_3$ (19 µL, 0.08 mmol). To this was added 5 mL of toluene. The pressure tube was sealed under nitrogen and heated at 110 ºC for 72 h. After this period, the pressure tube was cooled to room temperature. Subsequently, toluene was evaporated and reaction was quenched with water. The organic contents were extracted with chloroform, and the combined extract was dried over anhyd Na_2SO_4 and filtered. The solvent was removed in vacuo and the crude product was subjected to neutral alumina-column chromatography using ethyl acetate/pet. ether (30:70) as an eluent to yield pure **TB1** as a white powder, 0.35 g (67% yield); IR (film) cm^{-1} 3055, 2924, 1593, 1488, 1392, 1206; ^{1}H NMR ($CDCl_3$, 500 MHz) δ 3.95 (d, J = 16.5 Hz, 2H), 4.23 (s, 2H), 4.48 (d, J = 16.5 Hz, 2H), 6.60 (s, 2H), 6.86-6.92 (m, 10H), 7.14 (t, J = 8.5 Hz, 4H), 7.28-7.35 (m, 4H), 7.45 (t, J = 8.9 Hz, 4H), 7.75 (d, J = 7.9 Hz, 2H), 7.87 (d, J = 8.5 Hz, 2H), 7.91(d, J = 8.5 Hz, 2H); ^{13}C NMR ($CDCl_3$, 125 MHz) δ 58.3, 66.8, 120.2, 120.8, 120.9, 121.9, 124.2, 125.6, 126.1, 126.3 (×3), 127.2, 128.3, 128.4, 128.9, 131.2, 135.2, 142.3, 143.4, 144.3, 148.5; ESI-MS$^+$ *m/z* Calcd for $C_{47}H_{37}N_4$ 657.3018 $[M+H]^+$, found 657.3018.

Synthesis of TB2

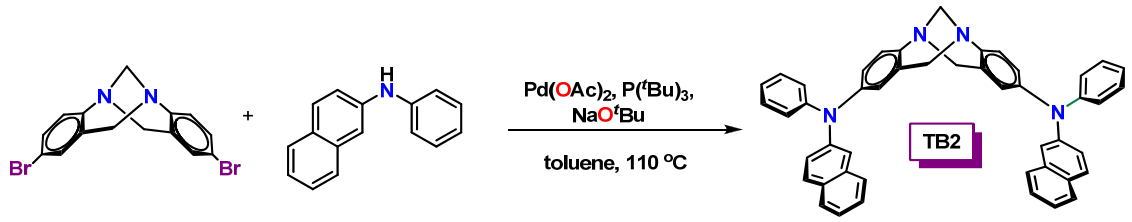

A similar C-N coupling protocol as described above for the synthesis of **TB1** was followed for the synthesis of **TB2** by employing 2,8-dibromo-substituted Tröger's base (0.30 g, 0.79 mmol), *N*-phenyl-2-naphthalenamine (0.42 g, 1.89 mmol). At the end of the reaction, solvent was removed in vacuo and the crude product was subjected to neutral alumina-column chromatography using ethyl acetate/pet. ether (30: 70) as an eluent to yield pure **TB2** as white powder (0.36 g, 69% yield); IR (film) cm^{-1} 3054, 2923, 1627, 1591, 1489, 1467, 1272; ^{1}H NMR ($CDCl_3$, 500 MHz) δ 4.03 (d, J = 16.5 Hz, 2H), 4.31 (s, 2H), 4.56 (d, J = 16.5 Hz, 2H), 6.71 (d, J = 2.0 Hz, 2H), 6.97-7.04 (m, 6H), 7.08 (d, J = 7.3 Hz, 4H), 7.22-7.26 (m, 6H), 7.32-7.40 (m, 6H), 7.56 (d, J = 8.5 Hz, 2H), 7.69 (d, J = 8.5 Hz, 2H) 7.74 (d, J = 7.9 Hz 2H); ^{13}C NMR ($CDCl_3$, 125 MHz) δ 58.3, 66.9, 119.8, 122.4, 122.6, 123.94, 123.99, 124.2, 124.3, 125.8, 126.2, 126.8, 127.5, 128.6, 128.8, 129.2, 129.8, 134.3, 143.3, 143.6, 145.4, 147.7; ESI-MS^{+} *m/z* Calcd for $C_{47}H_{37}N_4$ 657.3018 $[M+H]^{+}$, found 657.3018.

Synthesis of TB3

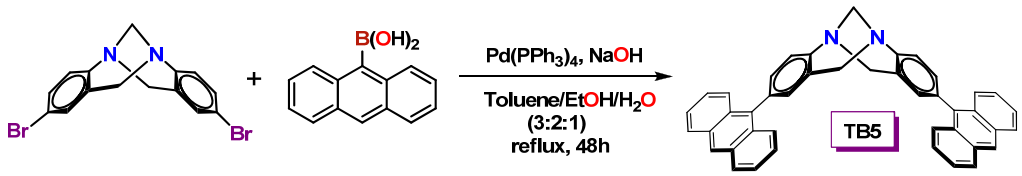

2,8-dibromo-substituted TB was subjected to Pd(0)-catalyzed Suzuki coupling with 9-anthraceneboronic acid. Thus, an oven-dried two-necked round-bottom flask was charged with dibromo-substituted TB (0.50 g, 1.3 mmol), 9-anthraceneboronic acid (1.75 g, 7.9 mmol), $Pd(PPh_3)_4$ (0.23 g, 0.20 mmol) and NaOH (0.42 g, 10.5 mmol) under N_2 atmosphere. The contents were dissolved in a 60 mL of toluene-EtOH-H_2O mixture (3:2:1) and heated at reflux for 48 h. After completion of the reaction, as monitored by thin-layer chromatography, the contents were evaporated to dryness in vacuo and the residue extracted with $CHCl_3$ and brine. The organic phase was dried over anhyd. Na_2SO_4 and concentrated in vacuo to obtain the crude product. Silica gel column chromatography was performed using $CHCl_3$/ pet. ether (25:75) as an eluent to obtain pure **TB3** as a colorless solid (0.57 g, 75 % yield); IR (solid) cm^{-1} 3047, 2899 1622, 1493, 1358, 1203; ^{1}H NMR ($CDCl_3$, 500 MHz) δ 4.44 (d, J = 17.1 Hz, 2H), 4.60 (s, 2H), 4.91 (d, J = 17.1 Hz, 2H), 7.09 (s, 2H), 7.29-7.49 (m, 12H), 7.67 (d, J = 9.2 Hz, 2H), 7.75 (d, J = 9.2, 2H), 8.05 (d, J = 8.6, 4H), 8.49 (s, 2H); ^{13}C NMR ($CDCl_3$, 125 MHz) δ 58.7, 67.1, 125.0, 125.12, 125.19, 125.30, 125.35, 126.5, 126.7, 126.8, 127.9, 128.3, 128.4, 129.6, 130.2, 130.3, 131.3, 134.3, 136.6, 147.5; EI-MS^+ *m/z* Calcd for $C_{43}H_{31}N_2$ 575.2487 $[M+H]^+$, found 575.2485.

Synthesis of TB4

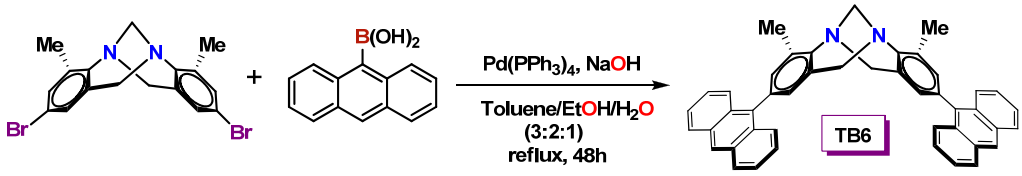

2,8-dibromo-4,10-dimethyl-substituted TB (2,8-dibromo-4,10-dimethyl-6*H*,12*H*-5,11-methanodi-benzo[*b*,*f*][1,5]-diazocine) was synthesized by following the literature reported procedure.[1] A similar Pd(0)-catalyzed Suzuki coupling protocol as described above for the synthesis of **TB3** was followed for the synthesis of **TB4** by employing dibromo-substituted TB (0.50 g, 1.22 mmol), 9-anthraceneboronic acid (1.63 g, 7.35 mmol), $Pd(PPh_3)_4$ (0.28 g, 0.24 mmol) and NaOH (0.39 g, 9.8 mmol). At the end of the reaction, solvent was removed in vacuo and the crude product was subjected to neutral alumina-column chromatography using $CHCl_3$/pet. ether (25:75) as an eluent to obtain pure product as a colorless solid (0.51 g, 70 % yield); IR (solid) cm^{-1} 2922, 2849, 1734, 1622, 1474, 1363, 1212; ^{1}H NMR ($CDCl_3$, 400 MHz) δ 2.51 (s, 6H), 4.25 (d, J = 16.9 Hz, 2H), 4.58 (s, 2H), 4.80 (d, J = 16.9 Hz, 2H), 6.94 (s, 2H), 7.17 (s, 2H), 7.36-7.47 (m, 8H), 7.73 (d, J = 8.7 Hz, 2H), 7.79 (d, J = 8.7, 2H), 8.02-8.06 (m, 4H), 8.48 (s, 2H); ^{13}C NMR ($CDCl_3$, 125 MHz) δ 17.2, 55.0, 67.8, 125.04, 125.07, 125.2, 126.9, 127.0, 127.1, 128.0, 128.32, 128.37, 130.2, 130.3, 131.3, 131.8, 132.9, 134.0, 137.0, 145.5; EI-MS^+ *m/z* Calcd for $C_{45}H_{35}N_2$ 603.2800 $[M+H]^+$, found 603.2797.

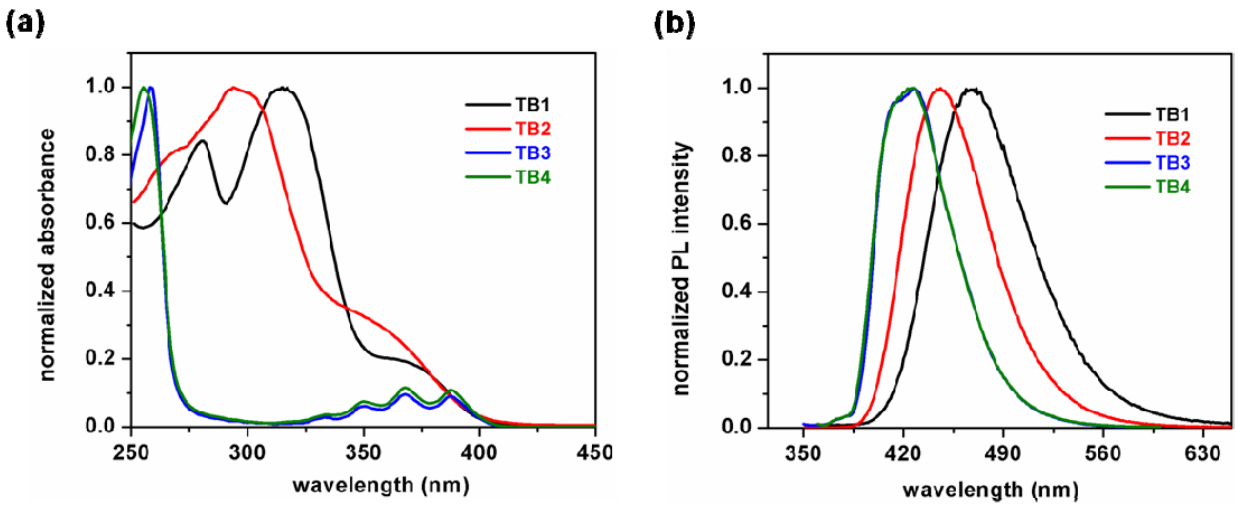

Figure S1. Normalized absorption (a) and PL spectra (b) of all **TB1-4** in 10^{-5} M DCM solutions.

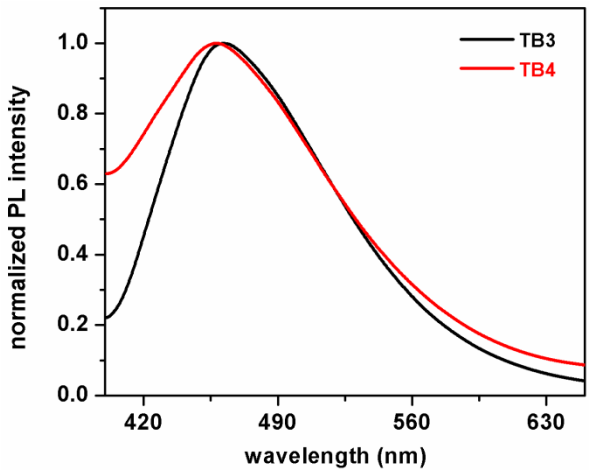

Figure S2. PL emission spectra of vacuum sublimed films of **TB3** and **TB4** when excited at 360 nm.

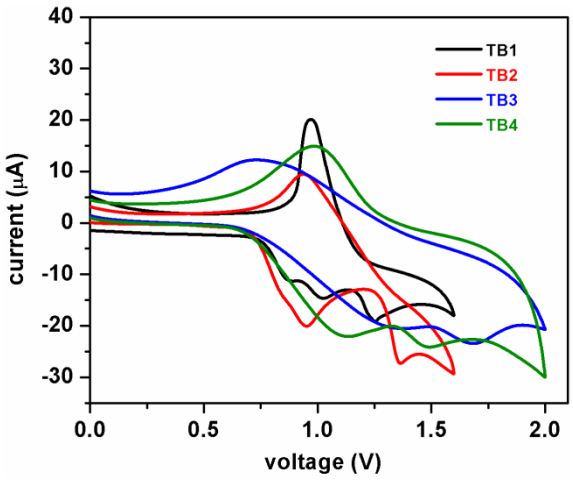

Figure S3. Cyclic voltammograms of **TB1-4** in DCM using *n*-Bu_4NPF_6 as the supporting electrolyte.

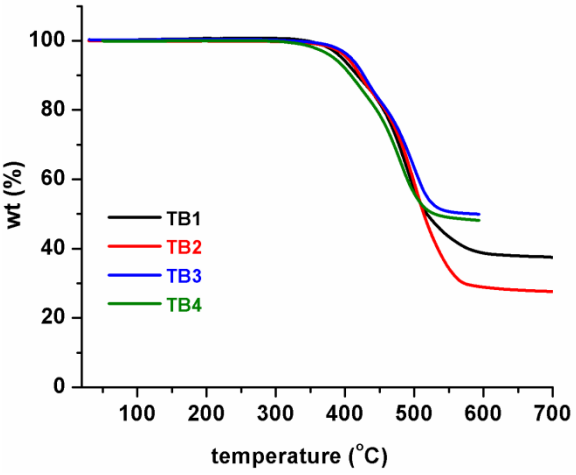

Figure S4. TGA profiles of **TB**s.

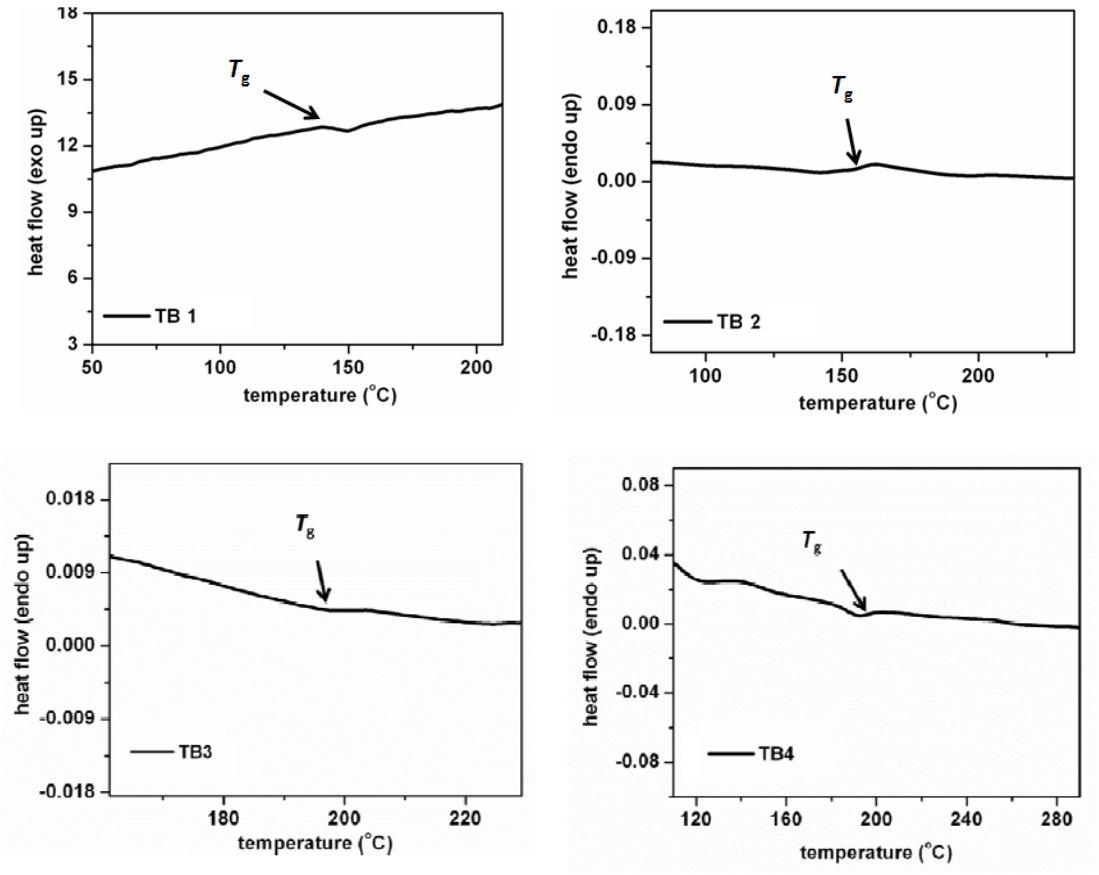

Figure S5. DSC profiles of **TB1-4**.

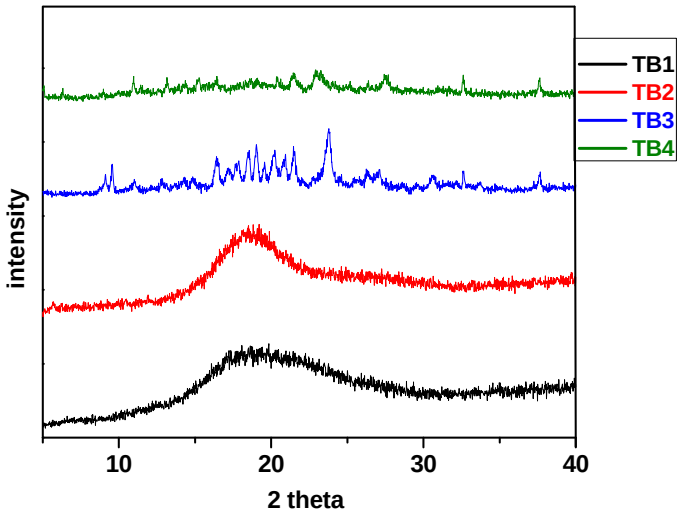

Figure S6. The powder X-ray diffraction profiles of **TB**s.

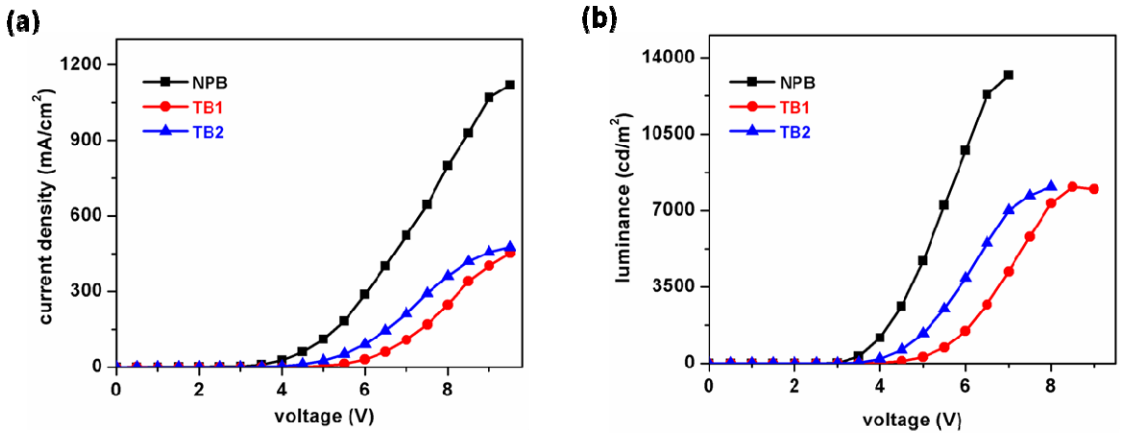

Figure S7. Plots of current density vs. voltage (a) luminance vs. voltage (b) for the devices constructed using **TB1-2** and **NPB** as HTMs and TPA as an EM, refer to text.

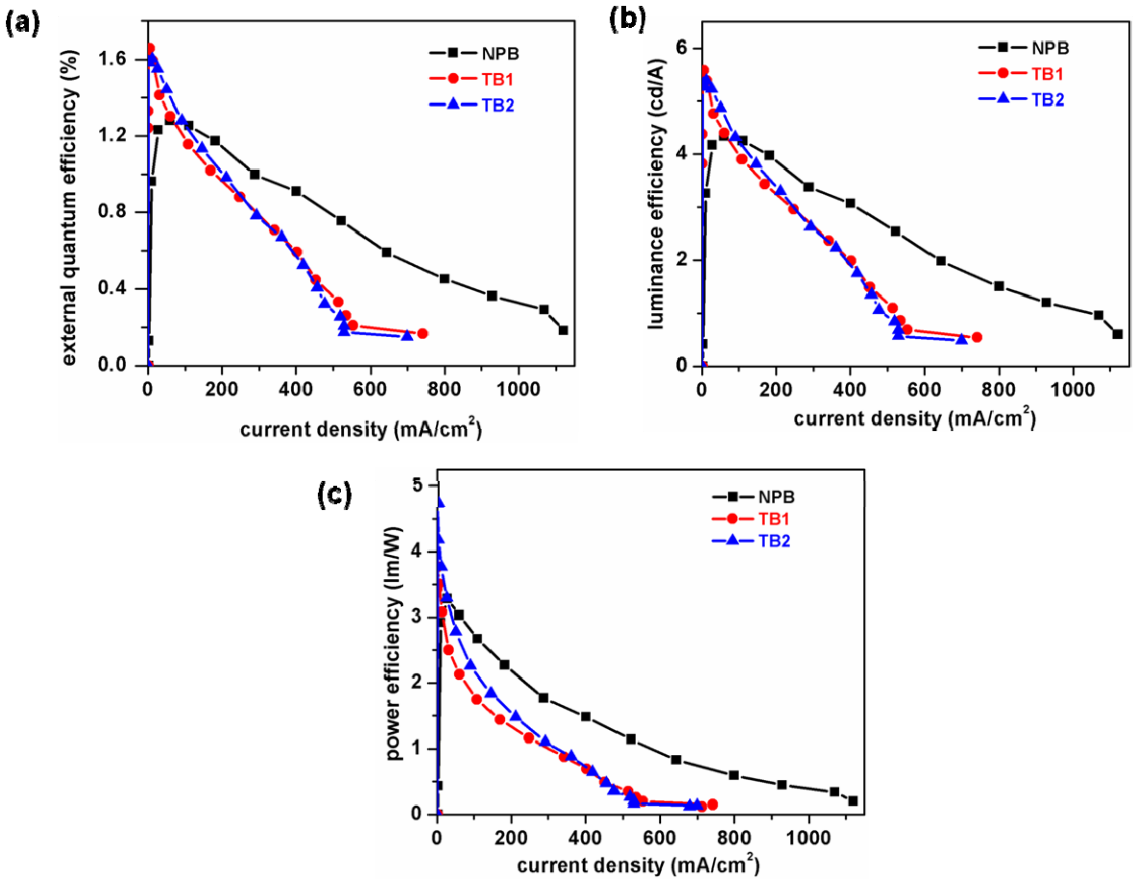

Figure S8. Plots of external quantum efficiency vs. current density (a), luminance efficiency vs. current density (b) and power efficiency vs. current density (c) for the devices of **TB1-2** and NPB as HTMs and TPA as an EM, refer to text.

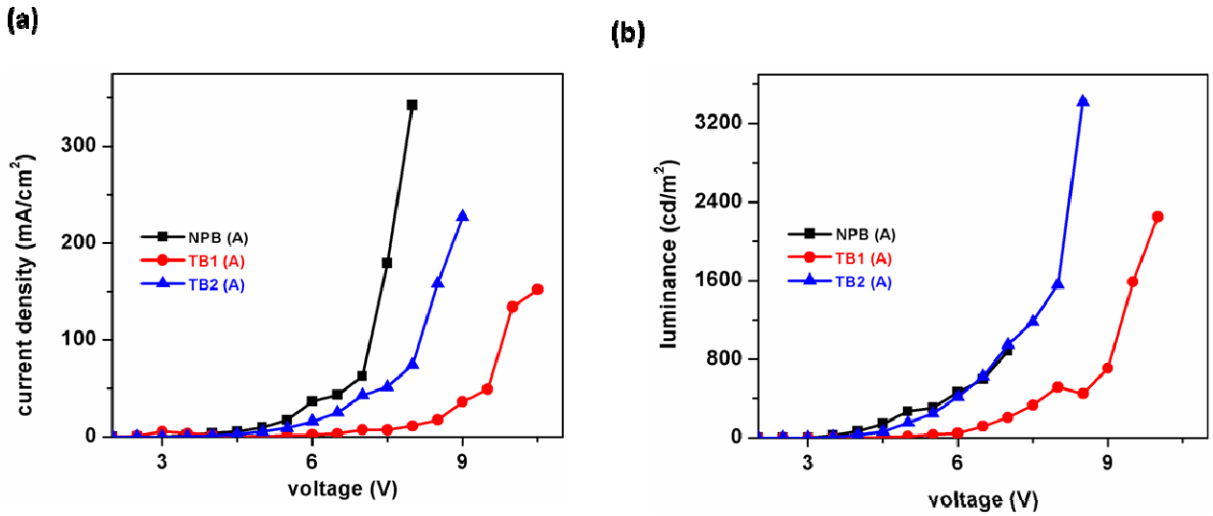

Figure S9. Plot of current density vs. voltage (a) and luminance vs. voltage (b) for the devices constructed using **TB**s and **NPB** as HTMs with **TB3** as an EM.

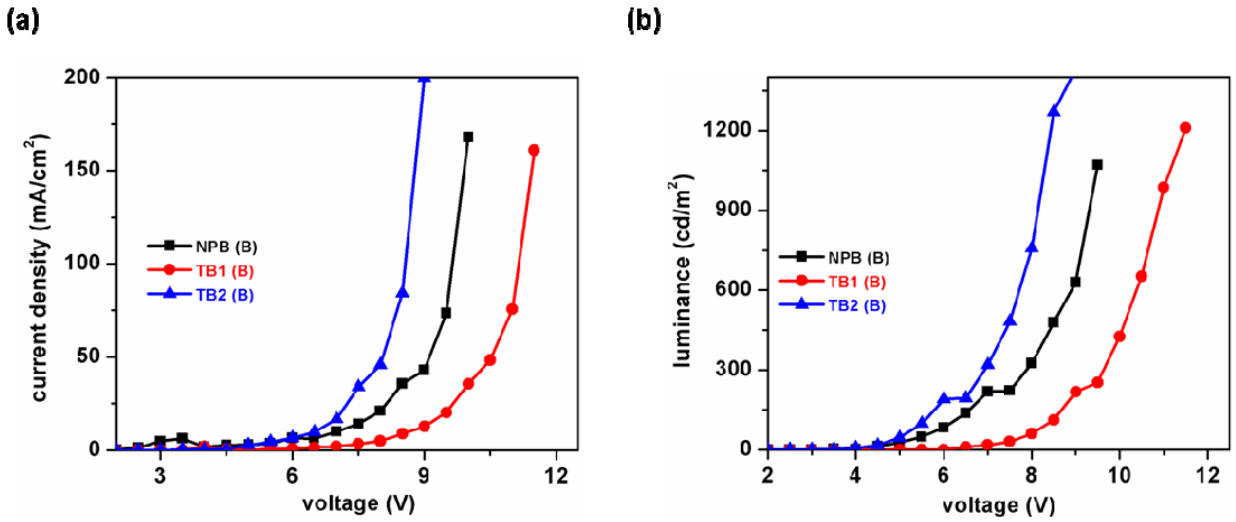

Figure S10. Plot of current density vs. voltage (a) and luminance vs. voltage (b) for the devices constructed using **TB**s and **NPB** as HTMs with **TB4** as an EM.

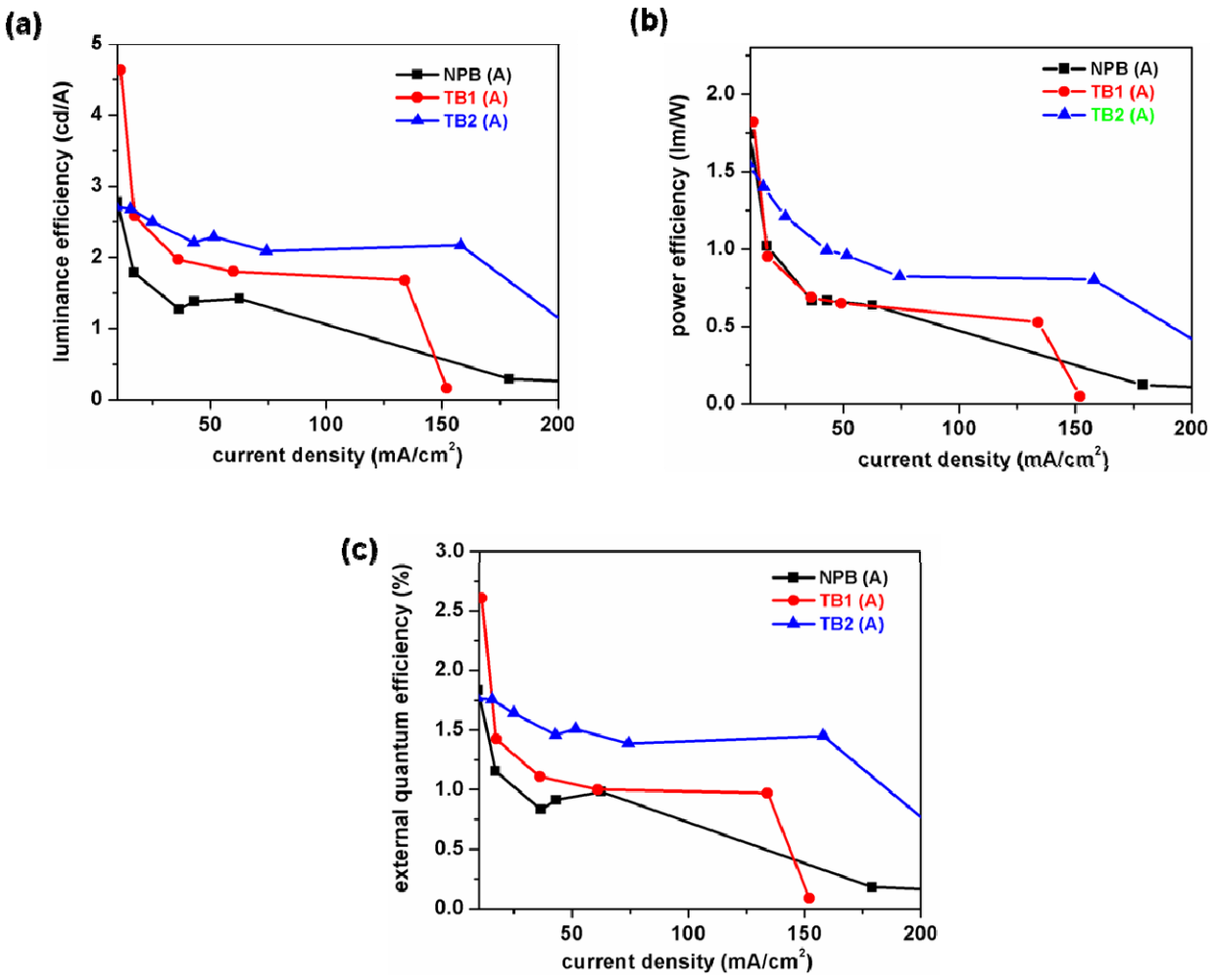

Figure S11. Plots of luminance efficiency vs. current density (a), power efficiency vs. current density (b) and external quantum efficiency vs. current density (c) for the devices of **TB1-2** and NPB as HTMs with **TB3** as an EM, i.e., for device configuration A, refer to text.

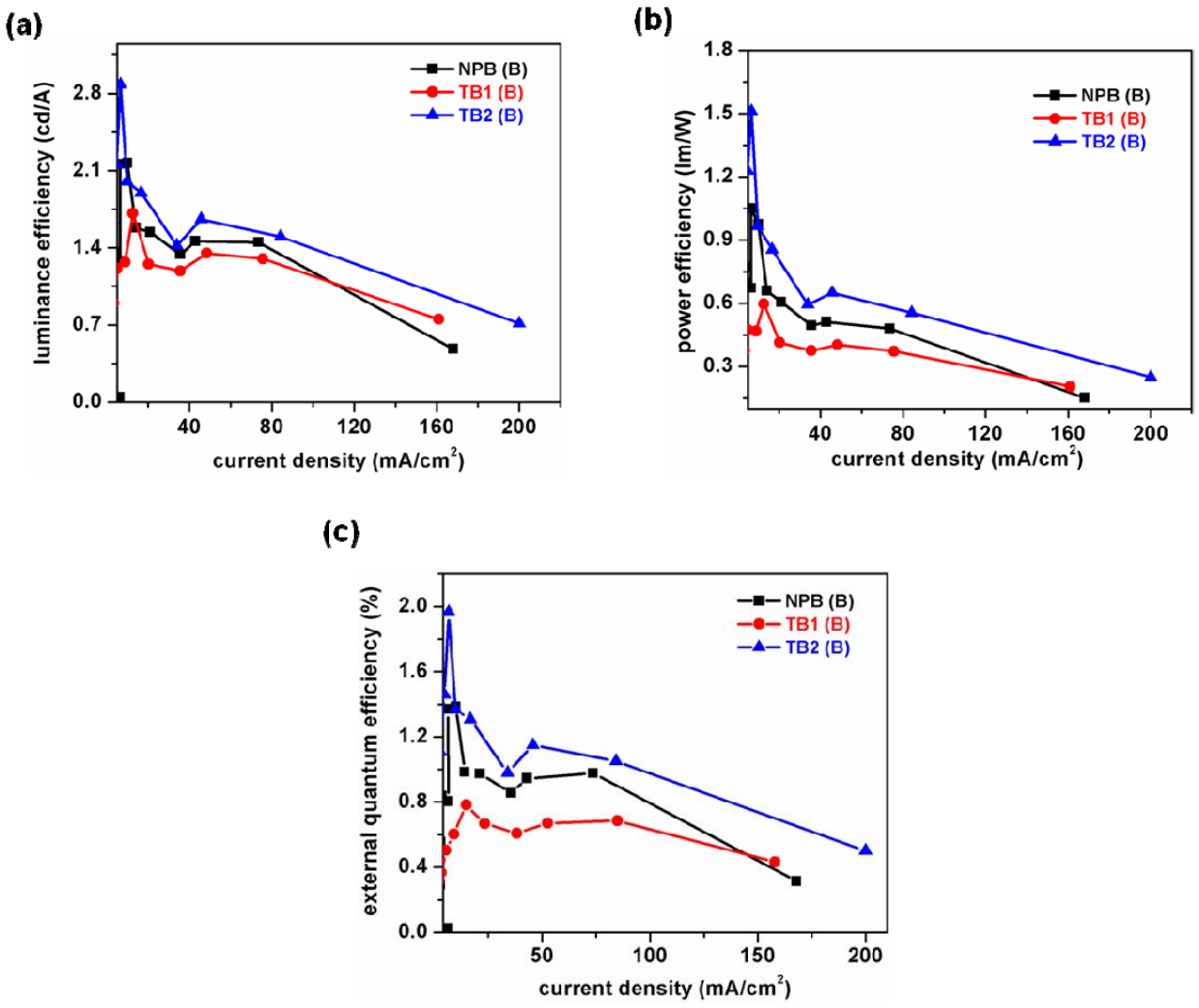

Figure S12. Plots of power efficiency vs. current density (a), luminance efficiency vs. current density (b) and external quantum efficiency vs. current density (c) for the devices of **TB**s and NPB with device configuration B, refer to text.

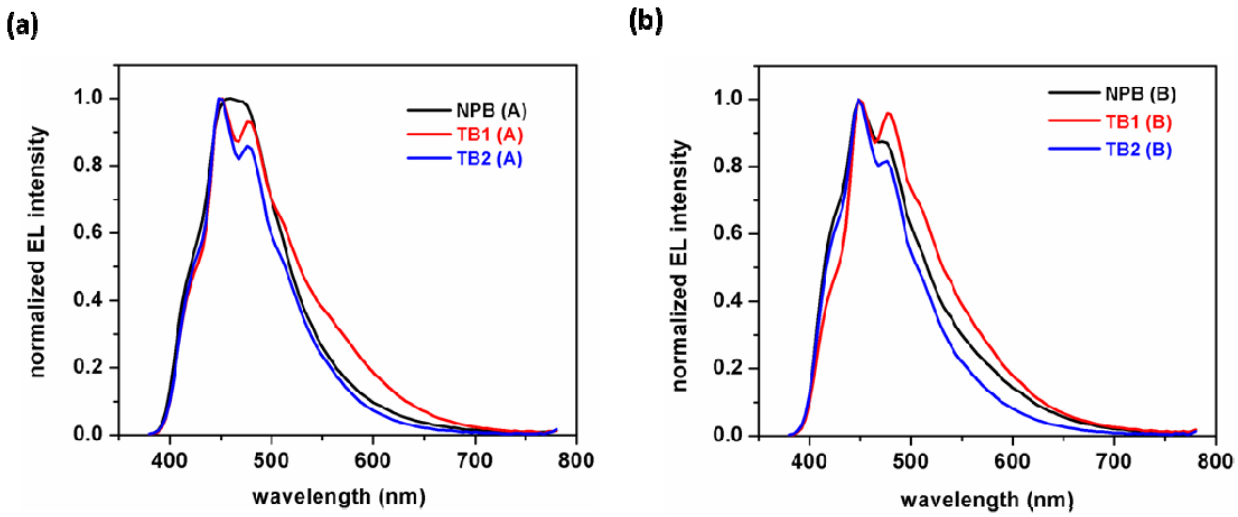

Figure S13. EL spectra captured from the devices of **TB**s and NPB in configuration A (a) and in configuration B (b).

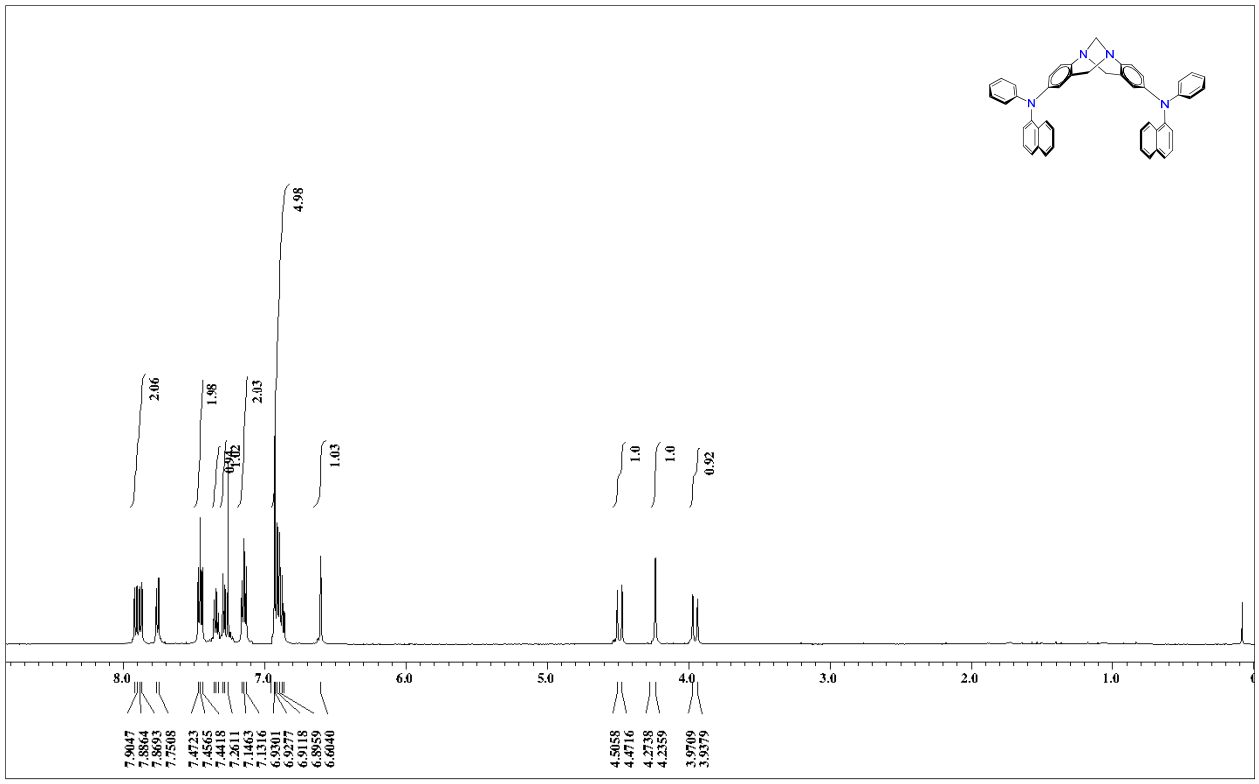

Figure S14. ^{1}H NMR spectrum (500 MHz, $CDCl_3$) of **TB1**.

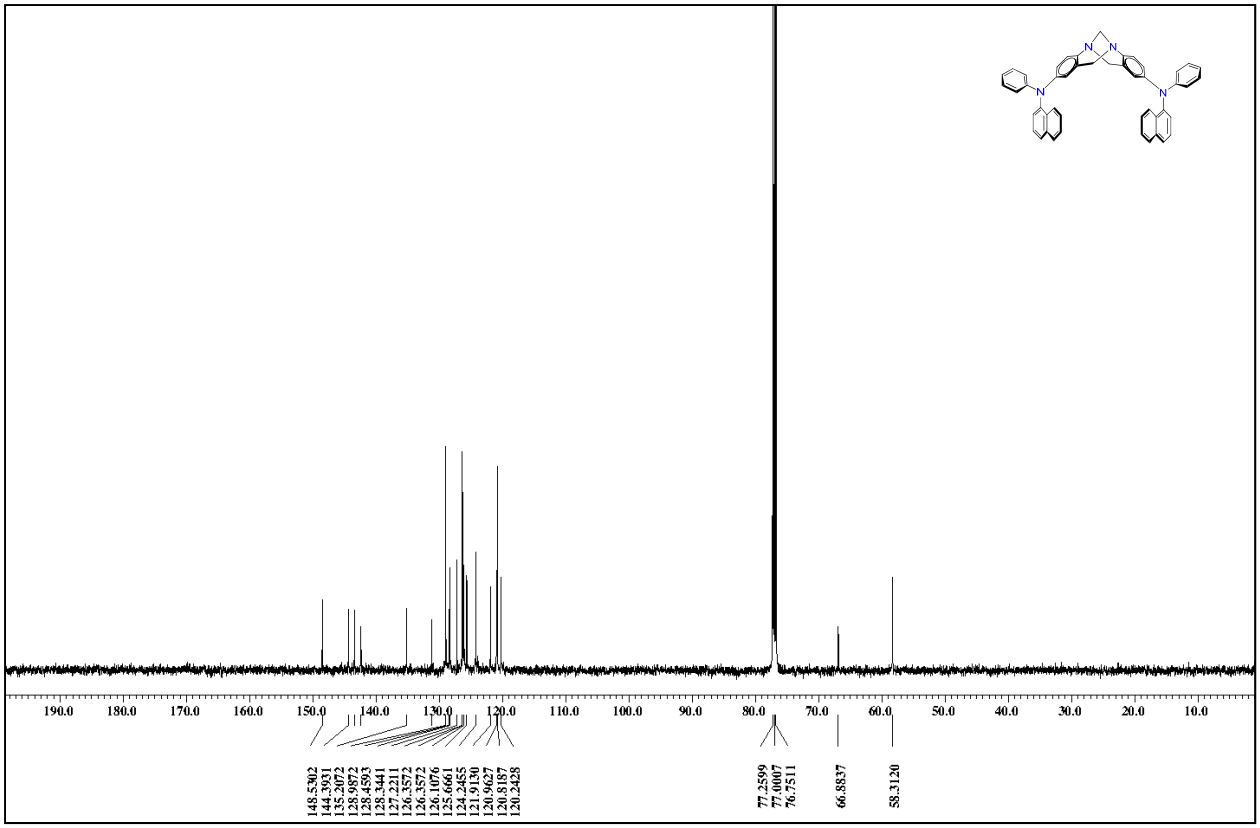

Figure S15. ^{13}C NMR spectrum (125 MHz, $CDCl_3$) of **TB1**.

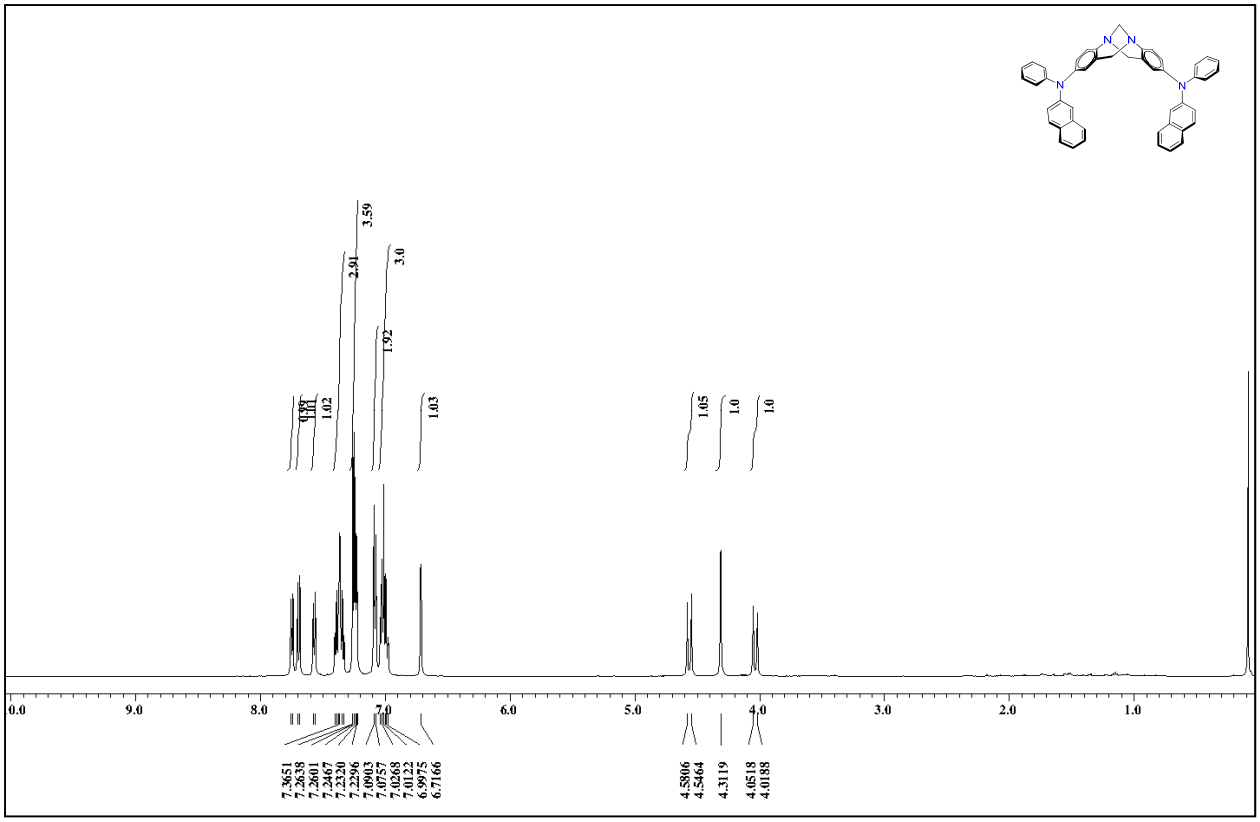

Figure S16. ^{1}H NMR spectrum (500 MHz, $CDCl_3$) of **TB2**.

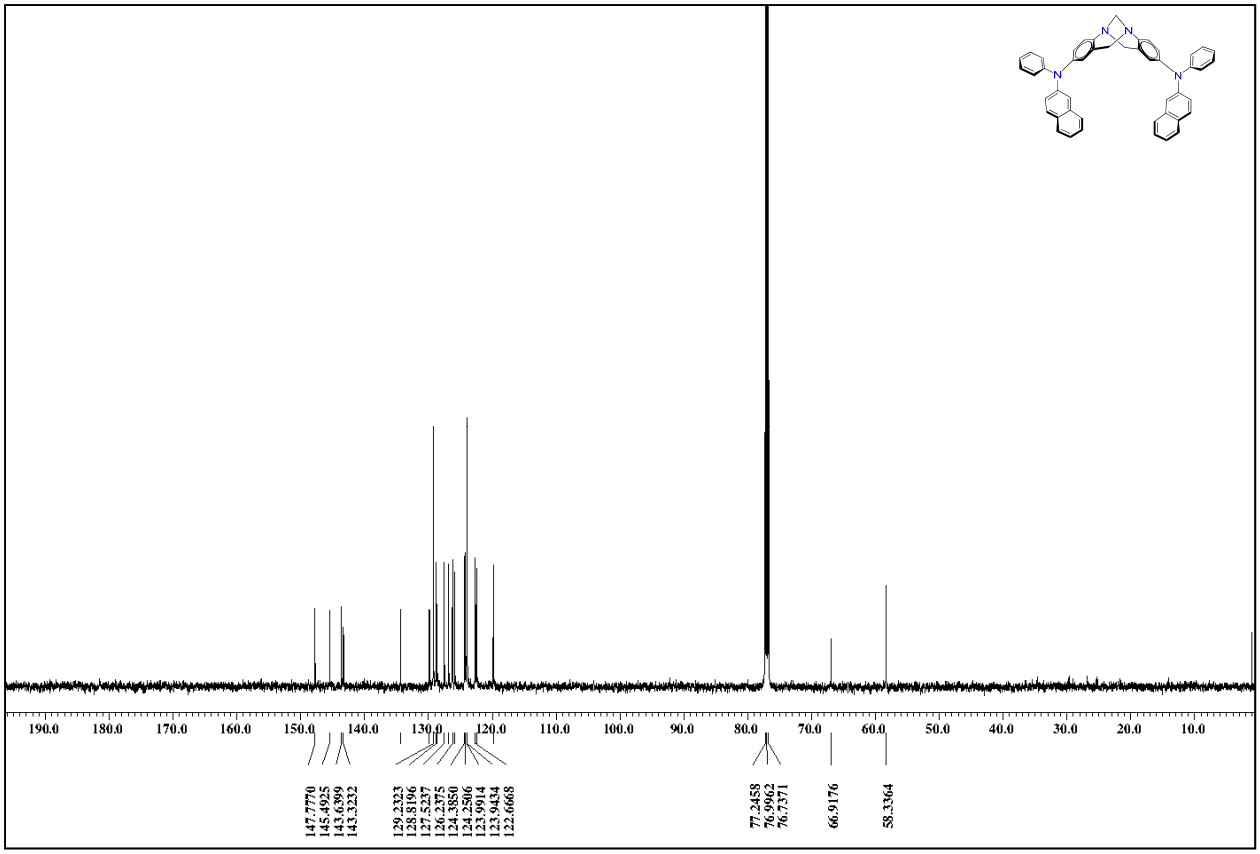

Figure S17. ^{13}C NMR spectrum (125MHz, $CDCl_3$) of **TB2**.

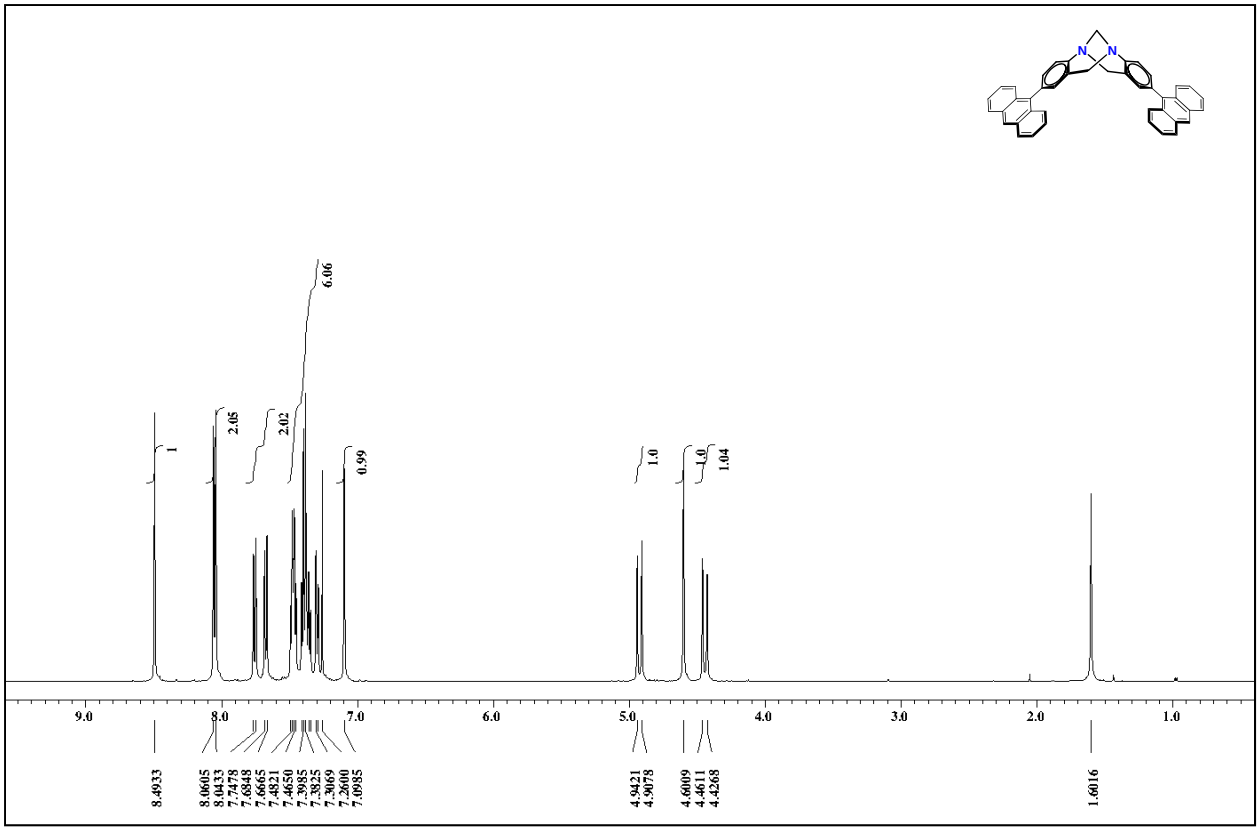

Figure S18. ^{1}H NMR spectrum (500 MHz, $CDCl_3$) of **TB3**.

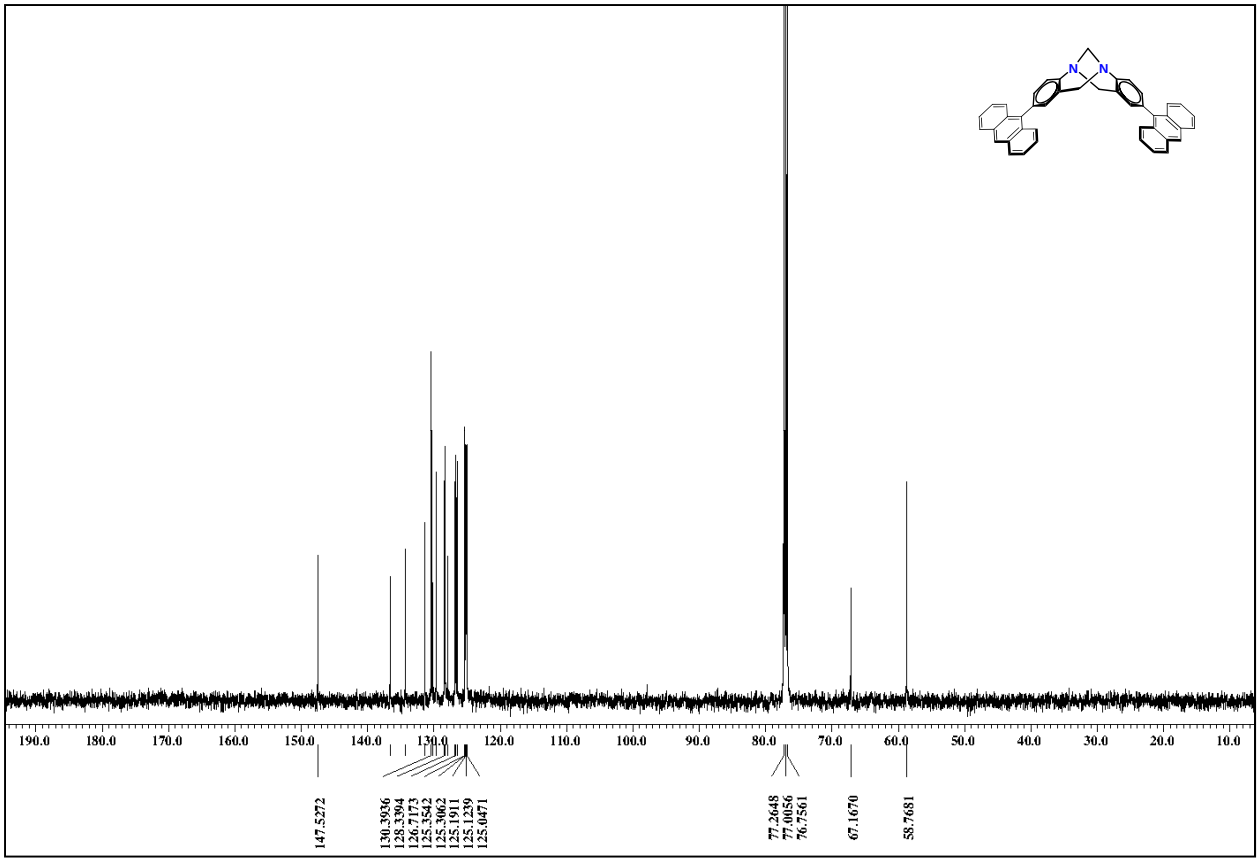

Figure S19. ^{13}C NMR spectrum (125 MHz, $CDCl_3$) of **TB3**.

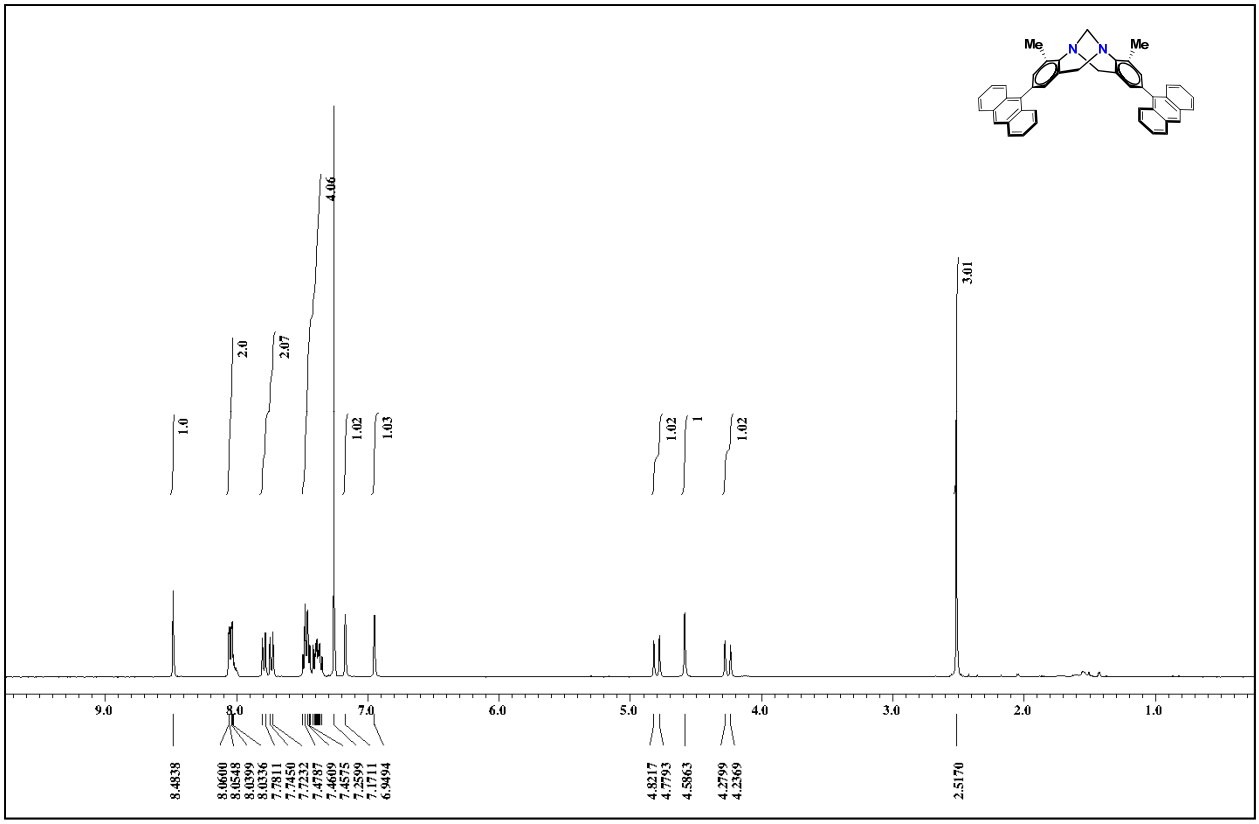

Figure S20. ^{1}H NMR spectrum (400 MHz, $CDCl_3$) of **TB4**.

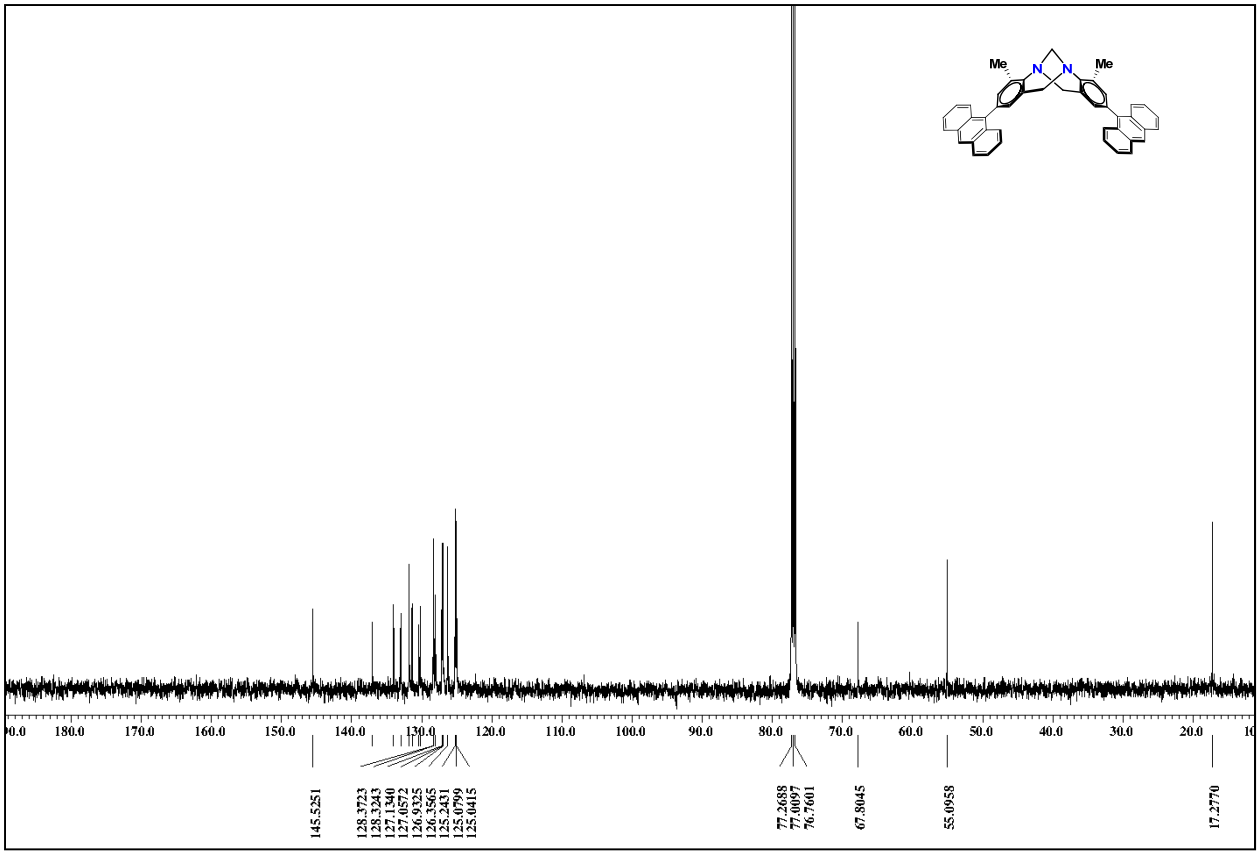

Figure S21. ^{13}C NMR spectrum (125 MHz, $CDCl_3$) of **TB4**.

References

1. J. Jensen, M. Strozyk and K. Wärnmark, *J. Heterocyclic Chem.* 2003, **40**, 373.
2. J. F. Hartwig, M. Kawatsura, S. I. Hauck, K. H. Shaughnessy and L. M. A. Roman, *J. Org. Chem*. 1999, **64**, 5575.